https://doi.org/10.15407/ujpe66.8.708

V.R. GAYEVSKII,[1] V.Z. KOCHMARSKII,[1] S.G. GAYEVSKA [2]

[1] National University of Water Management and Nature Resources Use
(11, Soborna Str., Rivne 33028, Ukraine; e-mails: v.r.haievskyi@nuwm.edu.ua, v.z.kochmarskii@nuwm.edu.ua)

[2] Rivne Research Forensic Center of the Ministry of Internal Affairs of Ukraine
(39, Gagarina Str., Rivne 33003, Ukraine; e-mail: gsg1979@ukr.net)

THE SURFACE ENERGY AND STRUCTURE OF NUCLEI AT CALCIUM SULFATE DIHYDRATE CRYSTALLIZATION FROM AQUEOUS SOLUTIONS

Crystallization of $CaSO_4 \cdot 2H_2O$ at the varying Ca^{2+} and the constant SO_4^{2-} ion concentrations has been studied. It is found that the concentration of $CaSO_4^0$ complexes can exceed the concentration of Ca^{2+} ions, which influences the crystallization conditions, in particular, the supersaturation. Based on the induction period measurements, the surface energy of nuclei was determined. This parameter was found to change within an interval of 6.4–10.8 mJ/m^2 depending on the ratio between the concentrations of Ca^{2+} ions and $CaSO_4^0$ complexes. We assume that the surface energy value depends on the prenucleus formation conditions. We adopt that prenuclei are micelles the nuclei of which undergo the recharging when passing from $C_{Ca^{2+}} < C_{SO_4^{2-}}$ to $C_{Ca^{2+}} > C_{CaSO_4^0} > C_{SO_4^{2-}}$.

Keywords: crystallization, surface energy, concentrations of components, induction period, micelles, photometry.

1. Introduction

The study of the crystallization mechanism of low soluble salts has both fundamental (the phase transition mechanism) and application (resistance to the salt deposition onto technological surfaces) importance [1–4]. When analyzing the formation of solid-phase nuclei in electrolytes, the value of the surface energy plays an important role, because it governs the rate of solid phase generation, as well as our understanding of the mechanism of nucleus formation [5] and its influence on the process running with surfactants which are widely used to control the growth of deposits of insoluble salts in various industrial domains [4, 6–8].

The aim of this work was to determine the surface energy of nuclei by measuring the induction period at the crystallization of calcium sulfate dihydrate under the conditions, when the concentrations of reactants vary. We also intended to formulate a model of prenuclei (micelles) that further evolve into crystallization nuclei.

A wide-spread method to determine the surface energy is the induction period method based on the Gibbs–Volmer theory [9]. Its essence consists in the analysis of the dependence of the induction period t_i on the surface energy and the value of the supersaturation coefficient S in the initial solution. To an accuracy of lower-order terms, this dependence is given by the expression

$$\ln(t_i) = \frac{16\pi N_{\rm A} V_\mu^2}{3(RT)^3(\ln S)^2}\sigma^3 + \text{const}, \qquad (1)$$

where t_i is the induction period, N_A the Avogadro number, V_μ the molar volume, R the universal gas constant, T the thermodynamic temperature, and S the supersaturation coefficient.

As follows from this formula, in order to determine the surface energy, it is necessary, in addition to the induction period measurements, to calculate the supersaturation of the initial solution under experimental conditions.

2. Experimental Part

A specific feature of our research was the presence of the mode of quasicontinuous (with an interval of 10 s) measurement of the solution parameters (the calcium ion concentration, the light transmittance, and the temperature), which was provided by applying a computerized complex designed and manufactured for non-disturbing physicochemical studies at the Physico-Technological Laboratory of Water Systems (PTLWS) of the National University of Water Management and Nature Resources Use (NUWMNRU) [7, 10].

Crystallization was initiated by the mixing of $CaCl_2$ solutions with concentrations of 27.5, 30, 34, 40, 50, 52, 55, 60, 65, 75, and 100 mmol/dm^3 and the Na_2SO_4 solution with a concentration of 40 mmol/dm^3. The Na_2SO_4 solution was pre-poured into the reactor and thermostated to 25.1 °C. Then, the required amount of a $CaCl_2$ solution was dosed to the Na_2SO_4 solution in order to obtain the indicated concentrations. The solutions were stirred throughout the experiment. All solutions were prepared from reagents of the c.p. grade.

Since the induction period was most distinctly observed in experiments on light transmittance measurement, they were used in this work. The results of measurements after their initial mathematical processing are presented in Fig. 1. One can see a pronounced dependence of the induction period (the areas of the kinetic curve, where the light transmittance almost did not change), as well as the turbidity dynamics and depth, on the initial concentration of calcium ions. Such a behavior of the induction period takes place because the growing concentration of CaI^+ increases the probability of a cluster (micelle) formation from ions, as well as neutral and charged calcium-based complexes, which generally shortens the induction period and accelerates the formation of crystallization nuclei.

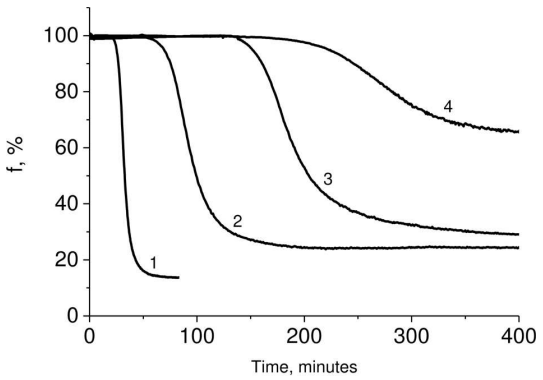

Fig. 1. Kinetic curves of the light transmittance f for the initial concentrations of Ca^{2+} ions $C^0_{Ca^{2+}}$ = 100 (*1*), 75 (*2*), 40 (*3*), and 34 mmol/dm^3 (*4*)

The initial stage of solid phase formation is characterized by a low consumption of calcium ions. However, the ionic composition of the solution may change due to rapid formation reactions of ionic complexes during the induction period.

3. Determination of the Solution Composition and Relative Supersaturation

To determine the current concentrations of Ca^{2+}, Na^+, SO_4^{2-}, and $NaSO_4^-$ ions, we used the balance equations for the molar component concentrations [8] and the electroneutrality equations:

$$C^0_{Ca^{2+}} = C_{Ca^{2+}} + C_{CaSO_4^0} + C_{CaSO_4^{hard}}, \quad (2)$$

$$C^0_{SO_4^{2-}} = C_{SO_4^{2-}} + C_{CaSO_4^0} + C_{NaSO_4^-} + C_{CaSO_4^{hard}}, \quad (3)$$

$$C^0_{Na^+} = C_{Na^+} + C_{NaSO_4^-}, \quad (4)$$

$$2C_{Ca^{2+}} + C_{Na^+} = 2C_{SO_4^{2-}} + C_{NaSO_4^-} + C_{Cl^-}. \quad (5)$$

In Eqs. (2) and (3), the notation $C_{CaSO_4^{hard}}$ means the solid phase concentration. We consider the processes within the limits of the induction period, so we may put $C_{CaSO_4^{hard}} \approx 0$ with an error less than 1%. Then, Eqs. (2) and (3) are simplified,

$$C^0_{Ca^{2+}} = C_{Ca^{2+}} + C_{CaSO_4^0}, \quad (6)$$

$$C^0_{SO_4^{2-}} = C_{SO_4^{2-}} + C_{CaSO_4^0} + C_{NaSO_4^-}. \quad (7)$$

To obtain a calculation procedure for the concentrations of the sulfate system components, let us assume that the formation time of the $NaSO_4^-$ and

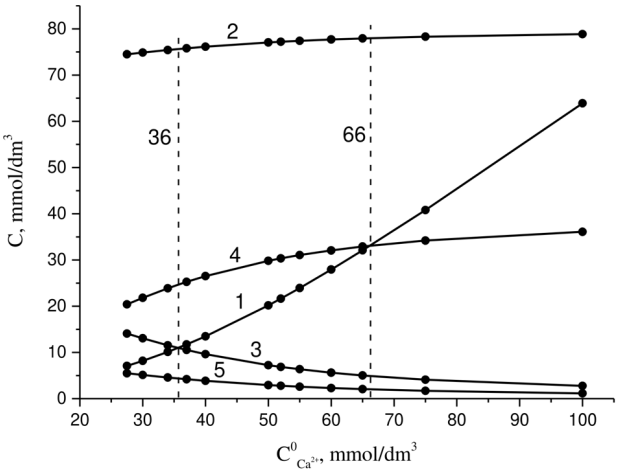

Fig. 2. Concentrations of the Ca^{2+}, Na^+, SO_4^{2-}, $CaSO_4^0$, and $NaSO_4^-$ components (curves *1* to *5*, respectively). The vertical dashed lines denote the equality points $C_{Ca^{2+}} = C_{SO_4^{2-}}$ and $C_{Ca^{2+}} = C_{CaSO_4^0}$. The interval $C^0_{Ca^{2+}} = 36 \div 66$ corresponds to $C_{SO_4^{2-}} < C_{Ca^{2+}} < C_{CaSO_4^0}$

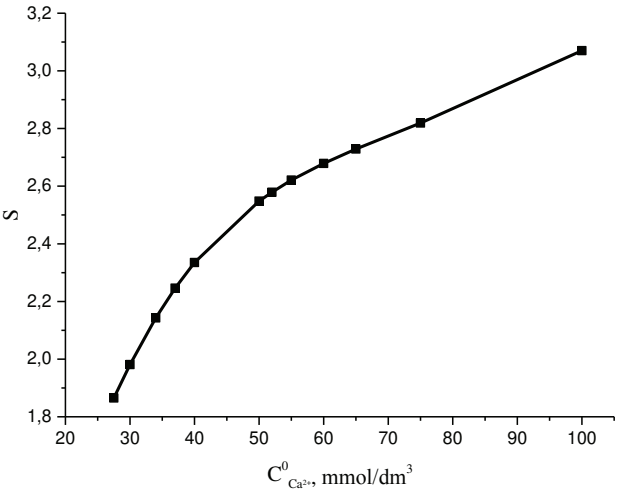

Fig. 3. Supersaturation dependence on the initial concentration of calcium ions

$CaSO_4^0$ complexes is much shorter than the induction period. So, we can apply the known equilibrium relations for the stability constants,

$$K_1 = \frac{C_{NaSO_4^-}}{C_{Na^+} C_{SO_4^{2-}}}, \quad K_2 = \frac{C_{CaSO_4^0}}{C_{Ca^{2+}} C_{SO_4^{2-}}}. \tag{8}$$

At $t = 25\ ^\circ C$, they equal $K_1 = 5.26 \times 10^{-3}$ dm^3/mol and $K_2 = 0.204$ dm^3/mol [11]. Together with Eqs. (4), (6), and (7), we obtain the following equation to calculate the concentration of SO_4^{2-} ions:

$$C^3_{SO_4^{2-}} + \left(a_2 + C^0_{Ca^{2+}}\right) C^2_{SO_4^{2-}} + \\ + \left(a_1 + \frac{1}{K_1} C^0_{Ca^{2+}}\right) C_{SO_4^{2-}} = \frac{1}{K_1 K_2} C^0_{SO_4^{2-}}, \tag{9}$$

$$a_1 = \frac{1}{K_1 K_2} + \left(\frac{1}{K_2} - \frac{1}{K_1}\right) C^0_{SO_4^{2-}}, \\ a_2 = \frac{1}{K_1} + \frac{1}{K_2} + C^0_{SO_4^{2-}}. \tag{10}$$

Solutions (10) and the concentrations of other components,

$$C_{Ca^{2+}} = \frac{C^0_{Ca^{2+}}}{1 + K_2 C_{SO_4^{2-}}}, \\ C_{Na^+} = \frac{C^0_{Na^+}}{1 + K_1 C_{SO_4^{2-}}} \tag{11}$$

are shown in Fig. 2. One can see that the concentration of free Ca^{2+} ions becomes higher than the concentration of $CaSO_4^0$ complexes only at the concentrations $C^0_{Ca^{2+}} > 66$ mmol/dm^3. At lower concentrations, the formation of nuclei is driven by sulfate complexes, and their properties (size, surface energy, solubility, density) have no stable values. To calculate the saturation state in the process of solid $CaSO_4 \cdot 2H_2O$ separation, we used the solubility product $Pr_{CaSO_4} = 1.0 \times 10^{-5}$ mol^2/dm^3 [12].

For the induction period, the supersaturation coefficient S was calculated according to Eq. (10),

$$S = \frac{(C_{Ca^{2+}} \gamma_{Ca^{2+}})(C_{SO_4^{2-}} \gamma_{SO_4^{2-}})}{Pr_{CaSO_4}}, \tag{12}$$

where γ_i are the activity coefficients. The latter were determined using the Davis formula [13]

$$-\lg(\gamma) = Z^2 \left(\frac{0.522\sqrt{\mu}}{1 + 1.5\sqrt{\mu}} - 0.2\mu\right), \tag{13}$$

where Z is the ion charge, and μ the ionic strength of the solution, which was calculated by the formula

$$\mu = 0.5(4C_{Ca^{2+}} + C_{Na^+} + 4C_{SO_4^{2-}} + C^0_{Cl^-}). \tag{14}$$

Note that, in all experiments, $C^0_{Cl^-} = 2C^0_{Ca^{2+}}$. The values of the activity coefficients for the doubly charged ions and the supersaturation coefficient S were determined by Eqs. (13) and (12), respectively, for various concentrations $C^0_{Ca^{2+}}$. The dependence of

the supersaturation coefficient S on the initial calcium concentrations is shown in Fig. 3.

The slope of the curve characterizes the rate of supersaturation decrease, and its variation testifies to different conditions for the formation of nuclei at low and high Ca^{2+} concentrations, which are reflected, in turn, in the surface energy dependence on $C^0_{Ca^{2+}}$.

4. Determination of Surface Energy

As was already mentioned, the surface energy was determined with the help of formula (1), which can be presented in the form

$$\ln(t_i) = \sigma^3 F(S) + \text{const}, \tag{15}$$

where

$$F(S) = \frac{A}{(\ln S)^2}, \quad A = \frac{16\pi N_A V_\mu^2}{3(RT)^3}, \tag{16}$$

and using the measurement data for the induction period, see Fig. 1. The interpolated dependences on the left- and right-hand sides of Eq. (13) change continuously. This fact makes it possible to select a discrete set of points in the interval of $C^0_{Ca^{2+}}$ variation, e.g.,

$$x_k = 27 + k, \quad k = 0, \tag{17}$$

and, taking the value of σ to be constant within the change interval $\Delta k = 1$, to calculate the surface energy as a function of the initial concentration $C^0_{Ca^{2+}}$, see Fig. 4.

$$\sigma_k = \sqrt[3]{\frac{\ln(ti_k) - \ln(ti_{k+1})}{F(S_k)F(S_{k+1})}}. \tag{18}$$

From Fig. 4, one can see that σ changes from $\sigma_1 = 6.4$ mJ/m^2 at $C^0_{Ca^{2+}} = 27.5$ mmol/dm^3 to $\sigma_2 = 10.8$ mJ/m^2 at $C^0_{Ca^{2+}} = 68$ mmol/dm^3. At $C^0_{Ca^{2+}} > 66$ mmol/dm^3, when the concentration of free calcium ions becomes higher than the concentration of ionic complexes $CaSO^0_4$, σ becomes practically constant (about 10.4 mJ/m^2) at $C^0_{Ca^{2+}} = 76$ mmol/dm^3. The average value of σ over the whole interval of $C^0_{Ca^{2+}}$ variation equals 8.5 mJ/m^2, which is close to a value of 8.4 mJ/m^2 obtained in work [14] and to a value of 4.98 mJ/m^2 obtained in work [6].

We connect the surface energy dependence on the concentration of calcium ions with a change in the

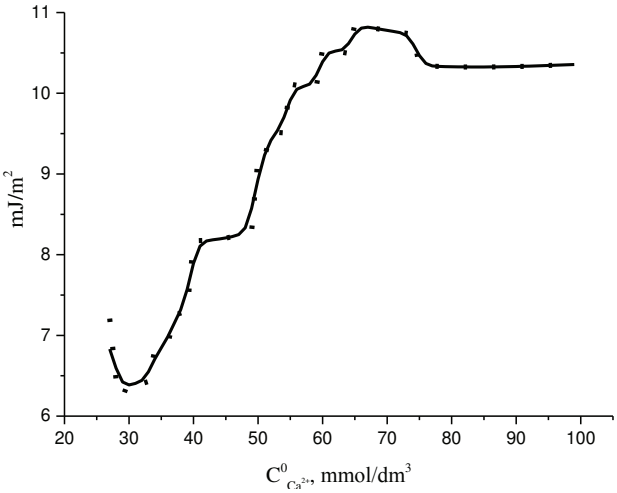

Fig. 4. Surface energy dependence on the initial calcium concentration. Symbols are the results of calculations by formula (18), and the curve is a result of the smoothing over 3 points

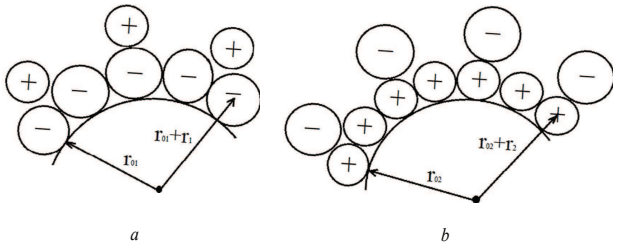

Fig. 5. Element of the core of a spherical micelle: the PDI is SO^{2-}_4 (*a*) or Ca^{2+} (*b*)

concentration of the potential-determining ion (PDI) in the micelle core (the micelle is considered to be a prenucleus of crystallization). When passing from $C^0_{Ca^{2+}} < C_{CaSO^0_4}$ to $C^0_{Ca^{2+}} > C_{CaSO^0_4}$, such a recharging is quite a natural phenomenon under the given conditions, which can occur according to the following schemes:

for $C^0_{Ca^{2+}} < C_{SO^{2-}_4}$ (Fig. 5, *a*),

$$m(CaSO_4)nSO^{2-}_4(n-x)Ca^{2+}xCa^{2+}; \tag{19}$$

for $C^0_{Ca^{2+}} > C_{SO^{2-}_4}$ (Fig. 5, *b*),

$$m(CaSO_4)nCa^{2+}(n-x)SO^{2-}_4xSO^{2-}_4. \tag{20}$$

Let the surface energy change be associated with the micelle core recharging (see Fig. 5). Then, it follows that the surface energy is determined by the electrical energy of the surface, which is proportional to the number of ions adsorbed on it. According to

Fig. 5, the maximum number of particles on the micelle surface, $N_{\max}$, depends on the PDI size (see Fig. 5, *a* for SO_4^{2-} and Fig. 5, *b* for Ca^{2+}) r_1 or r_2, and on the size r_{0_1} or r_{0_2} of micelles, which we consider as crystallization prenuclei. Then, for the spherical micelles, the numbers of adsorbed ions are equal to

$$N_{1\max} = \frac{4\pi(r_{01}+r_1)^2}{\pi r_1^2}, \quad N_{2\max} = \frac{4\pi(r_{02}+r_2)^2}{\pi r_2^2}, \tag{21}$$

and the electrostatic energy W of the micelle is determined by the known formula

$$W = \frac{q^2}{2C}, \tag{22}$$

where q is the charge of a sphere with radius R, and $C = 4\pi\varepsilon\varepsilon_0 R$ is its capacitance. Let us take into account that $q_1 = 2eb_1N_{1\max}$ and $q_2 = 2eb_2N_{2\max}$, where $e = 1.6\times10^{-19}$ C is the elementary charge, and b_1 and b_2 are coefficients that take into account how densely the ions fill the micelle surface.

By calculating the radii of micelles r_{01} and r_{02} in the framework of the Gibbs–Volmer theory,

$$r_{01} = \frac{2\sigma_1\mu}{RT\ln(S_1)\rho}, \quad r_{02} = \frac{2\sigma_2\mu}{RT\ln(S_2)\rho}, \tag{23}$$

where $\mu = 0.172$ kg is the molar mass, $\rho = 2320$ kg/m^3 is the density [11], $\sigma_1 = 6.4$ mJ/m^2, $\sigma_2 = 10.8$ mJ/m^2, and $S_1 = S_2 = 2.34$ (the value taken in a vicinity of $C^0_{Ca^{2+}} \approx C^0_{SO_4^{2-}}$), we obtain $r_{01} = 4.51\times10^{-10}$ m and $r_{02} = 7.61\times10^{-10}$ m. Using those values, taking the values $r_1 = 2.95\times10^{-10}$ m and $r_2 = 1.06\times10^{-10}$ m for the ion radii [15], on the basis of Eqs. (17) and (18), and assuming $b_1 \approx b_2$, we obtain

$$\frac{N_{2\max}}{N_{1\max}} = 1.5, \tag{24}$$

i.e. the number of Ca^{2+} ions adsorbed by micelles at $C^0_{Ca^{2+}} > C^0_{SO_4^{2-}}$ is larger than the number of SO_4^{2-} ions at $C^0_{Ca^{2+}} < C^0_{SO_4^{2-}}$. Taking Eqs. (18) and (19) into account, we see that the differences in the numbers of adsorbed Ca^{2+} and SO_4^{2-} ions testify that the surface energy change observed in the experiment is a result of the micelle recharging.

5. Conclusions

1. It has been shown that the limiting surface energy value equals $\sigma_1 = 6.4$ mJ/m^2 for the concentrations $C^0_{Ca^{2+}} < C^0_{SO_4^{2-}}$ and $\sigma_2 = 10.4$ mJ/m^2 for the concentrations $C^0_{Ca^{2+}} > C^0_{SO_4^{2-}}$. A wide interval of σ variation is connected with adsorption conditions for Ca^{2+} ions and micelle recharging, when the concentration $C^0_{Ca^{2+}}$ changes.

2. The surface energy dependence on $C^0_{Ca^{2+}}$ (see Fig. 4) is associated with a specific feature of the system $Ca^{2+} + SO_4^{2-} + 2H_2O$, which consists in a high concentration of $CaSO_4^0$ complexes (see Fig. 2, from which one can see that, at $C^0_{Ca^{2+}} < 66$ mol/dm^3, the concentration of complexes is higher than the concentration of Ca^{2+} ions). This situation affects the deposition of Ca^{2+} ions on the micelle surface and the micelle recharging in the course of prenucleus formation.

3. The average surface energy determined using the induction period value equals 8.5 mJ/m^2, which is consistent with the experimental data of other researchers (8.4 mJ/m^2 [14] and 4.98 mJ/m^2 [6]).

4. According to the micellar structure of prenuclei, which was proposed in this work, the dependence of their surface energy on the calcium concentration testifies that the formation of the surface, its structure, and the size of nuclei depend on the calcium concentration. In particular, the size of the nuclei should determine their other characteristics, e.g., solubility [16].

5. The analysis of experimental data with the assumption that micellar forms are prenuclei of the crystallization makes it possible to consider that, at the next stage of crystallization, the micelles will coagulate and create an amorphous form [5], which will turn later into a crystalline phase.

1. *Springer Handbook of Crystal Growth*, edited by G. Dhanaraj, K. Byrappa, V. Prasad, M. Dudley (Springer, 2010).
2. Zhilong Zhu, You Peng, T.A. Hatton, K. Samrane, A.S. Myerson, R.D. Braatz. Crystallization of calcium sulphate during phosphoric acid production: Modeling particle shape and size distribution. *Procedia Eng.* **138**, 390 (2016).
3. M. Mwaba, C. Rindt, A. van Steenhoven. Experimental investigation of $CaSO_4$ crystallization on a flat plate. *Heat Transf. Eng.* **27**, 42 (2006).
4. A.M. Pritchard. Deposition of hardness salts. In: *Fouling Science and Technology*. Edited by L.F. Melo, T.R. Bott, C.A. Bernardo (Kluwer, 1988), p. 261.

5. T.M. Stawski, A.E.S. van Driessche, M. Ossorio, J.D. Rodriguez-Blanco, R. Besselink, L.G. Benning. Formation of calcium sulfate through the aggregation of sub-3 nanometre primary species. *Nat. Commun.* **7**, 11177 (2016).
6. O.D. Linnikov. Investigation of the initial period of sulphate scale formation. Part 1. Kinetics and mechanism of calcium sulphate surface nucleation at its crystallization on a heat exchange surface. *Desalination* **122**, 1 (1999).
7. V.R. Gayevskyi, V.Z. Kochmarskyi. *Improving the Efficiency of Reversible Cooling Systems by Minimizing Calcium-Carbonate Deposits* (NUVGP, 2018) (in Ukrainian).
8. V. Kochmarskii, V. Melnyk. Formation of calcium carbonate from model solutions. Theoretical and experimental investigations. In: *Scientific Development and Achievements* (Science Publishing, 2018), Vol. 4, p. 138.
9. M. Volmer. *Kinetic der Phasenbildung* (Steinkopff, 1939).
10. V. R. Gajevskiy. Electric conductivity of carbon dioxide aqueous solutions. *Ukr. J. Phys.* **60**, 258 (2015).
11. L.G. Sillen, A.E. Martell, J. Bjerrum. *Stability Constants of Metal-Ion Complex* (Royal Society of Chemistry, 1964).
12. V.A. Rabinovich, Z.Ya. Khavin. *Brief Chemical Handbook* (Khimiya, 1978) (in Russian).
13. L. Meites. *Handbook of Analytical Chemistry* (McGraw Hill, 1963).
14. A. Hina, G.H. Nancollas, M. Grynpas. Surface induced constant composition crystal growth kinetics studies. The brushite-gypsum system. *J. Cryst. Growth* **223**, 213 (2001).
15. Ju. Lurie. *Handbook of Analytical Chemistry* (Mir Publishers, 1975).
16. V.Z. Kochmarskii, V.R. Gayevskii, N.L. Tyshko. Calcium carbonate crystallization from hydrocarbonate solution. *Ukr. J. Phys.* **62**, 382 (2017).

Received 30.06.20.
Translated from Ukrainian by O.I. Voitenko

В.Р. Гаєвський, В.З. Кочмарський, С.Г. Гаєвська

ПОВЕРХНЕВА ЕНЕРГІЯ ТА СТРУКТУРА ЗАРОДКІВ ПРИ КРИСТАЛІЗАЦІЇ ДИГІДРАТУ СУЛЬФАТУ КАЛЬЦІЮ З ВОДНИХ РОЗЧИНІВ

Досліджувалась кристалізація $CaSO_4 \cdot 2H_2O$ при зміні концентрації іонів Ca^{2+} і постійній концентрації SO_4^{2-}. Встановлено, що концентрація комплексів $CaSO_4^0$ може перевищувати концентрацію іонів Ca^{2+}, що впливає на умови кристалізації, зокрема, на перенасичення. За даними вимірювань індукційного періоду визначено поверхневу енергію зародків і встановлено, що вона змінюється в межах 6,4–10,8 мДж/м^2 залежно від співвідношення між концентраціями іонів кальцію і комплексів $CaSO_4^0$. Вважаємо, що величина поверхневої енергії залежить від умов формування протозародків. Приймаємо, що протозародками є міцели, ядра яких при переході від $C_{Ca^{2+}} < C_{SO_4^{2-}}$ до $C_{Ca^{2+}} > C_{CaSO_4^0} > C_{SO_4^{2-}}$ зазнають перезарядки.

Ключові слова: кристалізація, поверхнева енергія, концентрація компонентів, індукційний період, міцели, фотометрія.